



an ASME
publication

The Society shall not be responsible for statements or opinions advanced in papers or in discussion at meetings of the Society or of its Divisions or Sections, or printed in its publications. *Discussion is printed only if the paper is published in an ASME journal or Proceedings.*

Released for general publication upon presentation.

Full credit should be given to ASME, the Technical Division, and the author(s).

\$3.00 PER COPY

50 TO ASME MEMBERS

Dynamic Characteristics of Double-Pipe Heat Exchangers with Double Phase Change

M. SCHULT

Diplom-Ingenieur of Mechanical Engineering

F. MAYINGER

Professor of Mechanical Engineering

Technische Universität Hannover,
Institut Für Verfahrenstechnik,
Hannover, Federal Republic of Germany

The transfer function of a counter-flow heat exchanger by double-phase change is studied experimentally. The heat exchanger is a vertical channel of drawn stainless steel tubing. Freon 12 which is saturated flows from the bottom to the top of the tube and evaporates partially. The steam condenses in the annulus around it. Sinusoidal perturbations are impressed upon the mass flow of steam at the inlet of the test section. The responses of the mass flow of H₂O-condensate, freon 12-vapor, pressure drop of steam, and freon 12 are observed. Thermodynamic and hydrodynamic parameters are the mass flow, pressure, and inlet temperature of the undisturbed vaporization section. The results presented in transfer functions show that the dynamic characteristics of double-phase change are essentially determined by the flow-pattern and the temperature difference between the condensing side and the evaporating side.

Contributed by the Heat Transfer Division of The American Society of Mechanical Engineers for presentation at the Winter Annual Meeting, Atlanta, Georgia, November 27-December 2, 1977. Manuscript received at ASME Headquarters August 8, 1977.

Copies will be available until August 1, 1978.

Dynamic Characteristics of Double-Pipe Heat Exchangers with Double Phase Change

M. SCHULT

F. MAYINGER

ABSTRACT

The transfer function of a counter-flow heat exchanger by double-phase change is studied experimentally. The heat exchanger is a vertical channel of drawn stainless steel tubing. Freon 12 which is saturated flows from the bottom to the top of the tube and evaporates partially. The steam condensates in the annulus around it. Sinusoidal perturbations are impressed upon the mass flow of steam at the inlet of the test section. The responses of the mass flow of H₂O-condensate, freon 12-vapor, pressure drop of steam, and freon 12 are observed. Thermodynamic and hydrodynamic parameters are the mass flow, pressure, and inlet temperature of the undisturbed vaporization section. The results presented in transfer functions show that the dynamic characteristics of double-phase change are essentially determined by the flow-pattern and the temperature difference between the condensing side and the evaporating side.

NOMENCLATURE

A_{tfm}	= cross-sectional area of the turbine flow meter, m ²
A_f	= cross-sectional area of the inner tube, m ²
A_w	= cross-sectional area of the annulus, m ²
c_p^f	= specific heat of freon 12 at constant pressure, J/kg-K
c_p^w	= specific heat of water at constant pressure, J/kg-K
D	= damping coefficient
F	= transfer function
f	= frequency of oscillation, 1/s
\dot{M}_f	= mass flow rate of freon, kg/s
\dot{M}_w	= mass flow rate of water, kg/s
M_{st}	= steam mass stored in the system, kg
\dot{m}_f	= specific mass flow rate of freon, \dot{M}_f/A_f , kg/m ² -s
\dot{m}_w	= specific mass flow rate of water, \dot{M}_w/A_w , kg/m ² -s
pf	= system pressure on the evaporating side, bar
pw	= system pressure on the condensing side, bar
\dot{Q}	= exchanged heat between the condensing and the evaporating side

sf	= slip, velocity ratio of vapor and liquid, w_f/w_l
T	= time of oscillation, s
t	= time, s
V	= amplification coefficient, $ F $, $\Delta y_x / x_y$
w_f	= velocity of freon, m/s
x_o	= steady state value of the exciting function
\dot{x}_f	= quality of vapor, \dot{M}_f/\dot{M}_f
y_o	= steady state value of the response function
$\Delta h_{f_{lv}}$	= latent heat of the evaporation of freon, J/kg
$\Delta h_{w_{lv}}$	= latent heat of the evaporation of water, J/kg
$\Delta \dot{m}_{f_{vex}}$	= amplitude of the oscillating mass flow of vapor at the exit, kg/s
$\Delta \dot{m}_{w_{lex}}$	= amplitude of the oscillating mass flow of the condensate at the exit, kg/s
$\Delta \dot{m}_{w_{vin}}$	= amplitude of the oscillating mass flow of the steam at the inlet, kg/s
$\Delta(\Delta pf)$	= amplitude of the oscillating pressure drop on the evaporating side, bar
$\Delta(\Delta pw)$	= amplitude of the oscillating pressure drop on the condensing side, bar
Δx	= amplitude of the exciting oscillation
Δy	= amplitude of the oscillation of the response
$\Delta \vartheta_{f_{in}}$	= inlet subcooling of condensate, °C
$\Delta \vartheta_{w_{ex}}$	= outlet subcooling of condensate, °C
ϵ_f	= vapor void fraction
ϑ_f	= temperature of freon, °C
ϑ_w	= temperature of water, °C
ψ	= phase angle between the exciting oscillation and the oscillation of the response, deg.
ρ_f	= density of freon, kg/m ³
ω	= cyclic frequency, $2\pi/T$, 1/s
ω_w	= sharp cut off, 1/s

Subscripts

ex	= exit of the channel
in	= inlet of the channel
l	= liquid phase
lv	= mixture of liquid and vapor
o	= steady state

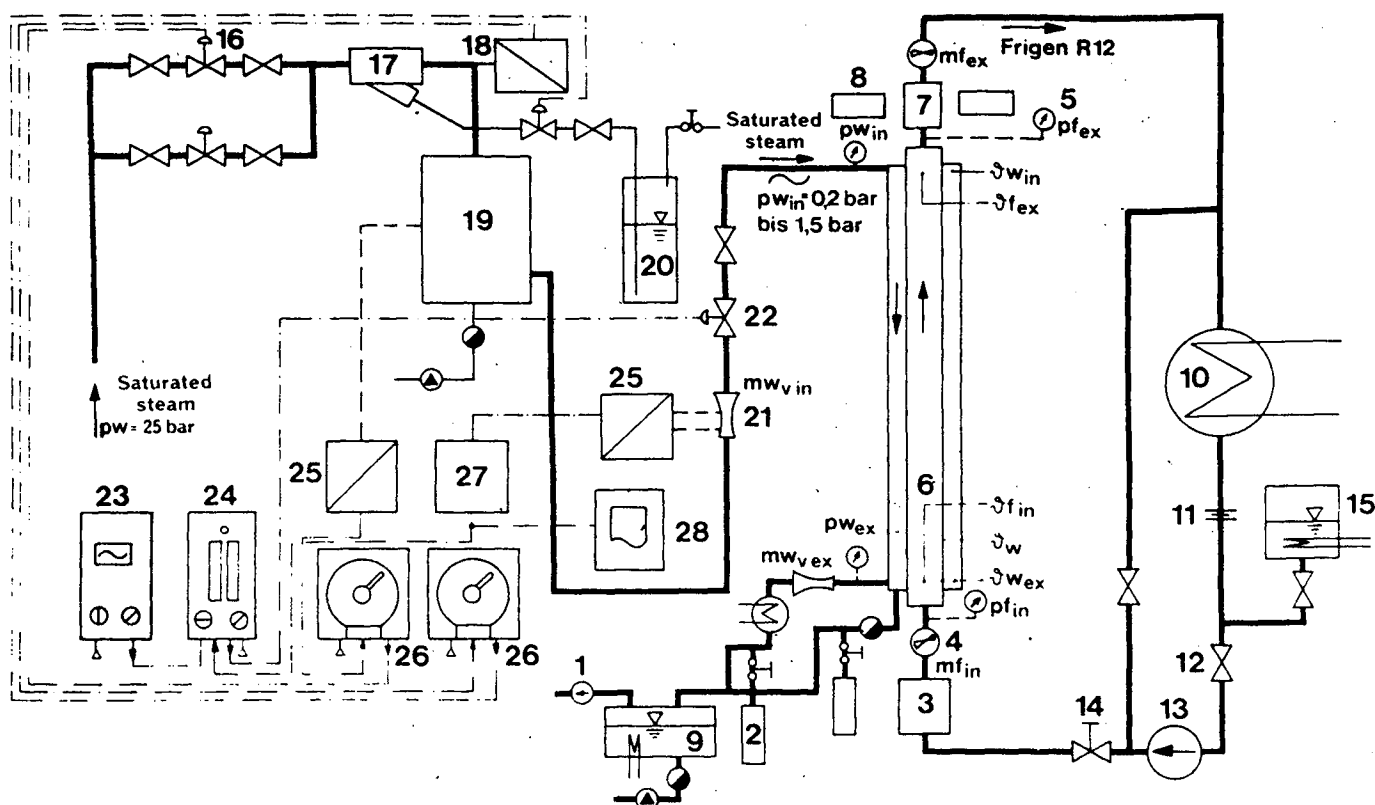


Fig. 1 Schematic of the coupled water-loop and freon R 12-loop

- | | |
|----------------------------------|---|
| (1) Vacuum pump | (15) Pressure holder |
| (2) Measurement of condensate | (16) Diaphragm control valve |
| (3) Preheater | (17) Injection cooler |
| (4) Turbine flow meter | (18) Measuring transmitter for temperature |
| (5) Measurement of pressure | (19) Buffer chamber |
| (6) Inner tube for R 12 | (20) Watertank for superheated steam cooler |
| (7) Gage glass | (21) Venturi tube |
| (8) Measurement of void fraction | (22) Diaphragm control valve |
| (9) Cooling water tank | (23) Pneumatic sinus transmitter |
| (10) Condenser | (24) PI-Controller |
| (11) Orifice | (25) Transmitter |
| (12) Valve | (26) PI-Controller |
| (13) Pump | (27) Square-root law transfer relays |
| (14) Control valve | (28) Pneumatic writer recorder |

v = vapor phase, steam phase
w = wall

INTRODUCTION

In power economy and chemical engineering heat exchangers with double phase change are often used for heat transfer. Heat exchangers with double phase change are also called steam transformers. In these a fluid is evaporated by condensing the same or another fluid.

The energy transfer by a two-phase flow has several advantages over that of a one-phase flow. One being, the fact that the heat transfer coefficient of a two-phase flow is usually greater than that of a one-phase flow. Therefore, an economical heat transfer is possible even when small temperature dif-

ference exists. A further advantage is that a smaller mass flow is required due to the latent heat of vaporization. Thus the dimensions of the circulation pump and the tubes can be kept smaller. In order to determine the design and the control of the steam transformers one must be acquainted with their dynamic behaviour. In double phase change the heat transfer and the hydrodynamics are closely connected. On both the condensing side and the evaporating side there is a two-phase flow. The steam quality is not only dependent on the heat transfer, but also on the flow resistance in the heat exchanging channels. Since both sides of the heat exchanger have a strong influence on each other, flow insta-

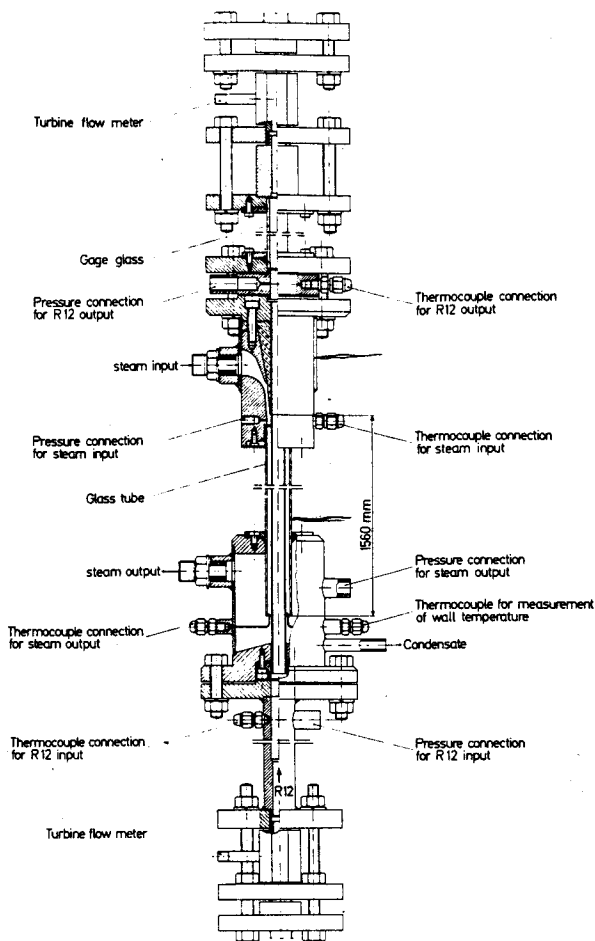


Fig. 2 Test section

bilities of one side produce a feedback effect on the flow of the other side. Sustained oscillations, however, can cause mechanical vibrations of the system and complicate the control of the condensate and vapor mass flow.

However, the study of the relevant literature shows that only little is known about the feedback effects and possible instabilities in double phase change. Three classes of possible flow oscillations have been defined and discussed in (1) and (2). To the first class belongs the "fundamental relaxation instability". This includes all flow instabilities may be classified that arise by a periodical change of bubble and annular flow. Between these two flow patterns there is a transitory region - the Churn-Flow -. If a heat exchanger operates in this region, flow instabilities may arise (3). It is not always clear, whether the periodical transition of the flow pattern is the cause of oscillations in density and pressure or whether the oscillations of density and pressure cause the transitions of the flow pattern (4), (5). In the second class one finds the "fundamental (or pure) dynamic instabilities". Here flow instabilities that are caused by density wave oscillations are grouped. Those

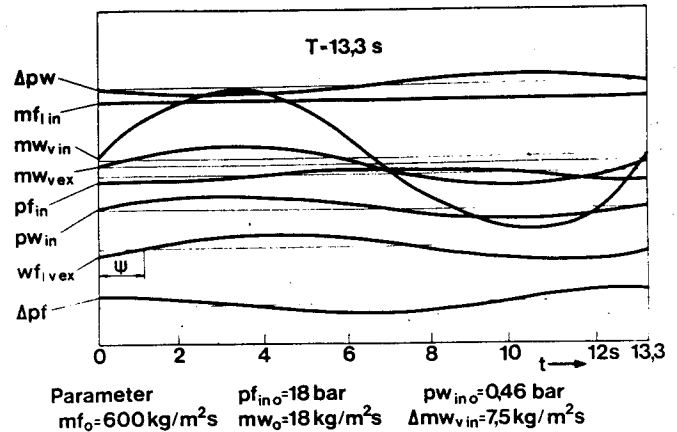


Fig. 3 Copy of a recording of the light beam oscilloscope (responses of mass flow, pressure and pressure drop)

oscillations can be induced by a disturbance of the mass flow rate (6), (7). Density wave oscillations can be very different. The dependence of the oscillating behaviour on the most important parameters, such as pressure, inlet subcooling, and mass flow rate was studied in ref. (8), (9).

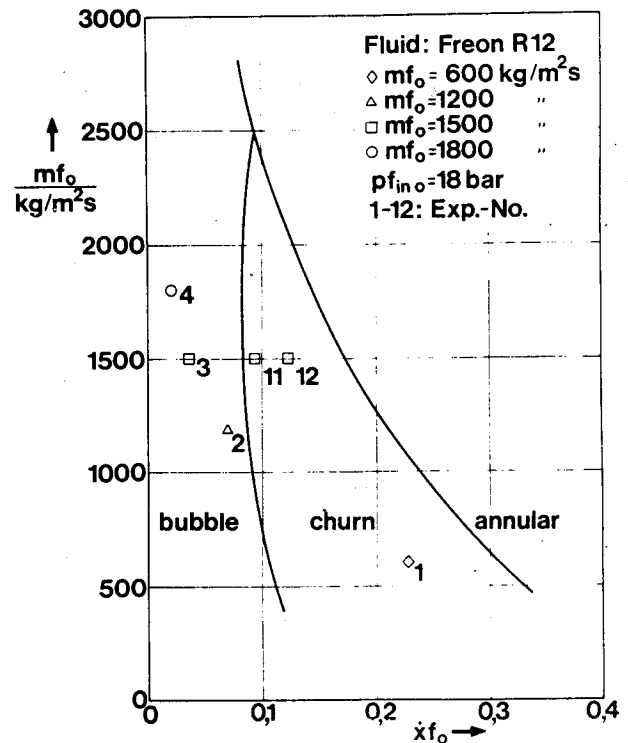


Fig. 4 Flow pattern map (12)

Table 1 Geometry of the test section

	inner tube	outer tube
outside diameter (mm)	15.0	26.0
thickness of the tube wall (mm)	0.5	2.0
roughness of the tube average value (μm)		
inside	2.5	
outside	1.2	
material	stainless steel V2A 1.4541	glass

length of the
test section: 1560 mm

annular clearance: 3.5 mm

The "compound dynamic instabilities" belong to the third class. This class includes the heat exchanger with double phase change instabilities. These can be traced back to the feed-back between the condensing and evaporating side by the two-phase friction pressure drops and heat transfers. This class also includes thermal oscillations which appear when the flow oscillates between film boiling and transition boiling.

The purpose of our investigations is to study the dynamic behaviour of heat exchangers with double phase change by aid of experiments. Based on experiments, a universal computer program shall be established, through which the transfer function and possible instabilities of heat exchangers with double phase change and their relationship to thermodynamic and hydrodynamic parameters, geometry and inclination can be quickly and reliably predicted.

During these experiments emphasis was placed on those disturbances which occur frequently in technical applications. The steam mass flow oscillations at the inlet of the heat exchanger belong to those disturbances.

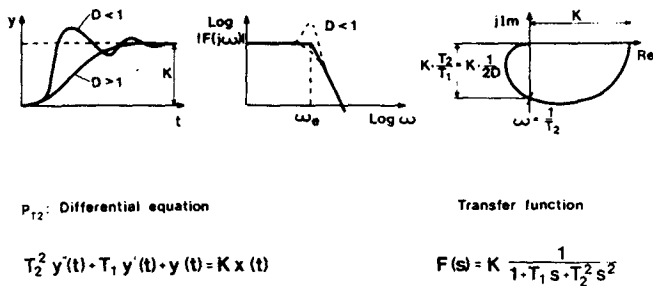


Fig. 5 Transient response and transfer function of a PT_2 -system

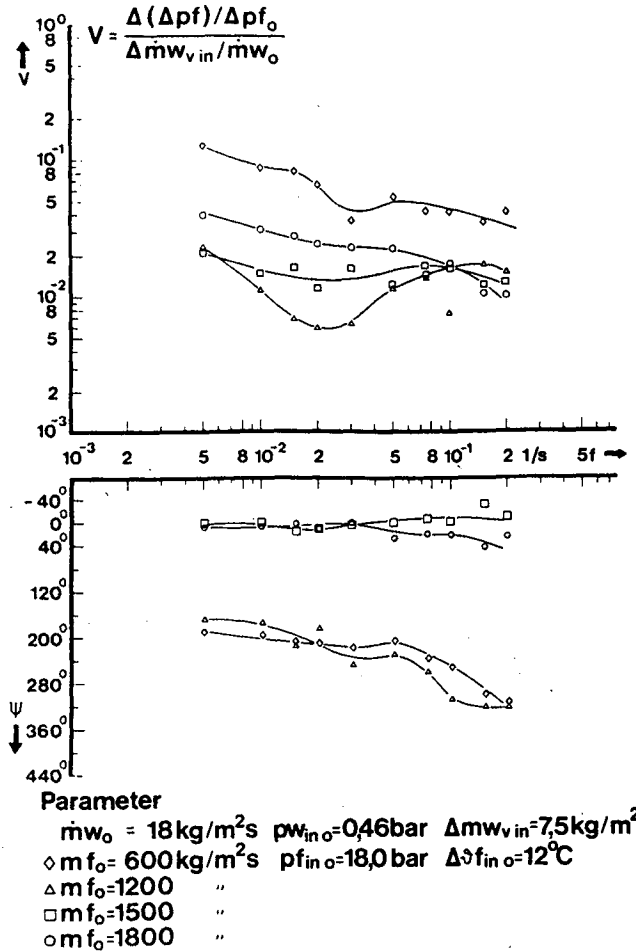


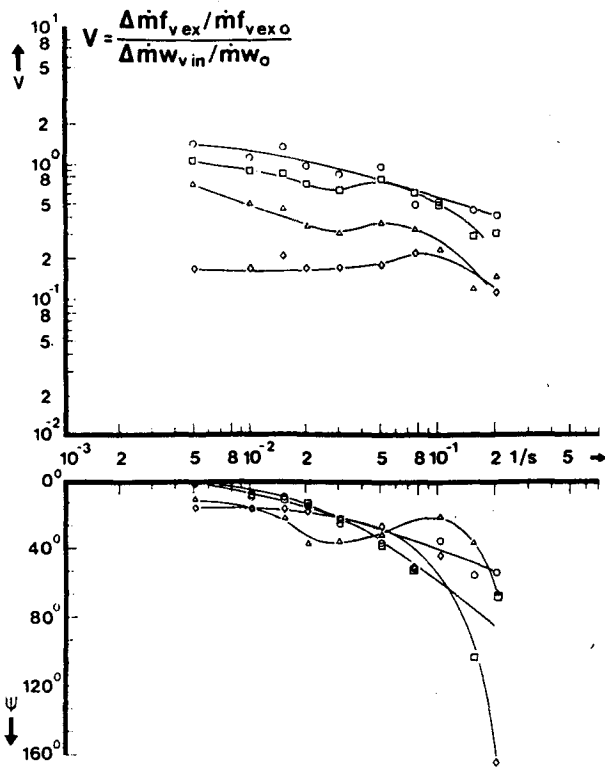
Fig. 6 Transfer functions of the test section in relation to the pressure drop on the evaporating side

By a periodical change of the steam mass flow the response functions and consequently, the transfer functions in relationship to the most important variables, condensate, vapour mass flow at the heat exchanger outlet, and pressure drop on both sides of the heat exchanger, could be examined. Parameters were the mass flow, the pressure and the inlet subcooling of the fluid on the undisturbed evaporating side. The mass flow of freon varied from 600 to 1800 $\text{kg/m}^2\text{s}$, the pressure of freon from 15 to 18 bar, and the degree of subcooling for the freon from 4 to 12 degree centigrade. But on the condensing side the stationary variables which were in a state of saturation, were the same for all experiments. The steam mass flow was on an average 18 $\text{kg/m}^2\text{s}$, the pressure was 0.46 bar, and the amplitude of steam mass flow oscillations was 7.5 $\text{kg/m}^2\text{s}$ (see Table 2).

EXPERIMENTAL STUDIES

Description of the Plant

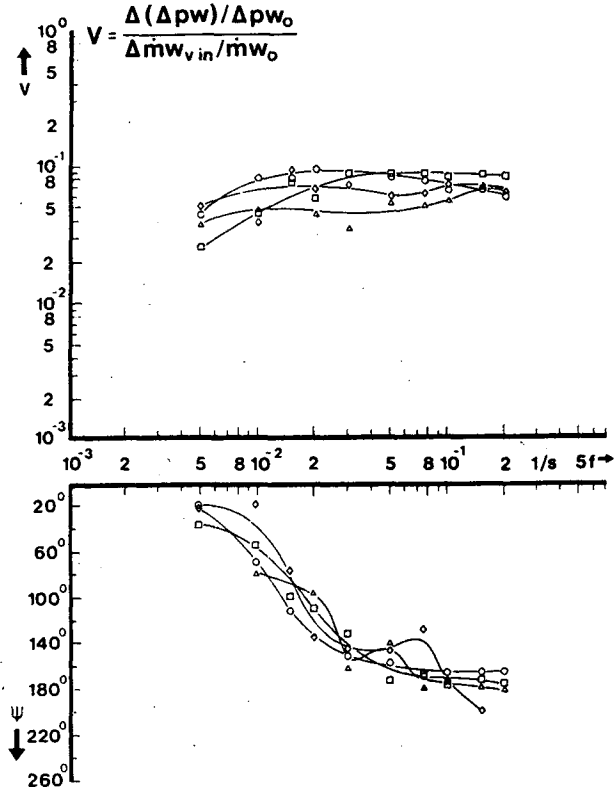
The schematic test set-up is shown in Fig. 1. The plant consists of a freon test loop - evaporation part - and of a water test



Parameter

$\dot{m}w_o = 18 \text{ kg/m}^2\text{s}$ $p_{w_{in}o} = 0.46 \text{ bar}$ $\Delta \dot{m}w_{vin} = 7.5 \text{ kg/m}^2\text{s}$
 $\diamond m_{f_o} = 600 \text{ kg/m}^2\text{s}$ $p_{fin o} = 18.0 \text{ bar}$ $\Delta \vartheta_{fin o} = 12^\circ\text{C}$
 $\triangle m_{f_o} = 1200$ "
 $\square m_{f_o} = 1500$ "
 $\circ m_{f_o} = 1800$ "

Fig. 7 Transfer functions of the test section in relation to the mass flow rate of vapor at the exit



Parameter

$\dot{m}w_o = 18 \text{ kg/m}^2\text{s}$ $p_{w_{in}o} = 0.46 \text{ bar}$ $\Delta \dot{m}w_{vin} = 7.5 \text{ kg/m}^2\text{s}$
 $\diamond m_{f_o} = 600 \text{ kg/m}^2\text{s}$ $p_{fin o} = 18.0 \text{ bar}$ $\Delta \vartheta_{fin o} = 12^\circ\text{C}$
 $\triangle m_{f_o} = 1200$ "
 $\square m_{f_o} = 1500$ "
 $\circ m_{f_o} = 1800$ "

Fig. 8 Transfer functions of the test section in relation to the pressure drop on the condensing side

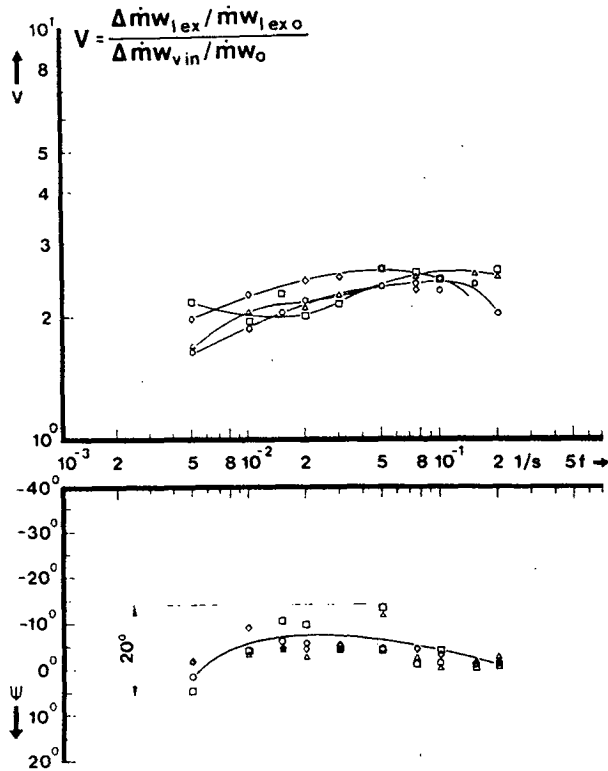
loop - condensation part. Both loops are coupled by a heat exchanger. For simple boundary conditions the heat exchanger consists of a vertical drawn, stainless steel tube which is placed concentrically in a glass tube (Fig. 2). Freon 12 flows from the bottom to the top of the stainless steel tube and partially evaporates. The steam which is flowing in the annular, condenses on the other side of the tube surface. Pump 13 transports the freon through the preheater 3, which controls the inlet temperature in the test section, to the heat exchanger. Table 1 shows the geometrical dimensions of the heat exchanger. The two-phase mixture freon is condensed and subcooled in condenser 10 and then flows back to pump 13.

On the condensing side saturated steam of 25 bar, produced by a steam generator, is reduced to the test conditions by means of diaphragm valve 16. The reduced superheated steam is cooled down to its saturation temperature by injection cooler 17. The sinusoidal perturbations are impressed upon the mass flow of steam at the inlet of the test section. PI-controller 24 serves the mass flow

control. This controller receives its nominal value from pneumatic sinus transmitter 23 and its actual value from the flow rate by a measurement of differential pressure at venturi tube 21. The signal of the command variable is transmitted to diaphragm valve 22. Due to the fact that not all of the steam directed to the test section is condensed, the two-phase mixture flows from the test section directly into a separator. The non-condensed steam is condensed in an external condenser.

Measuring technique

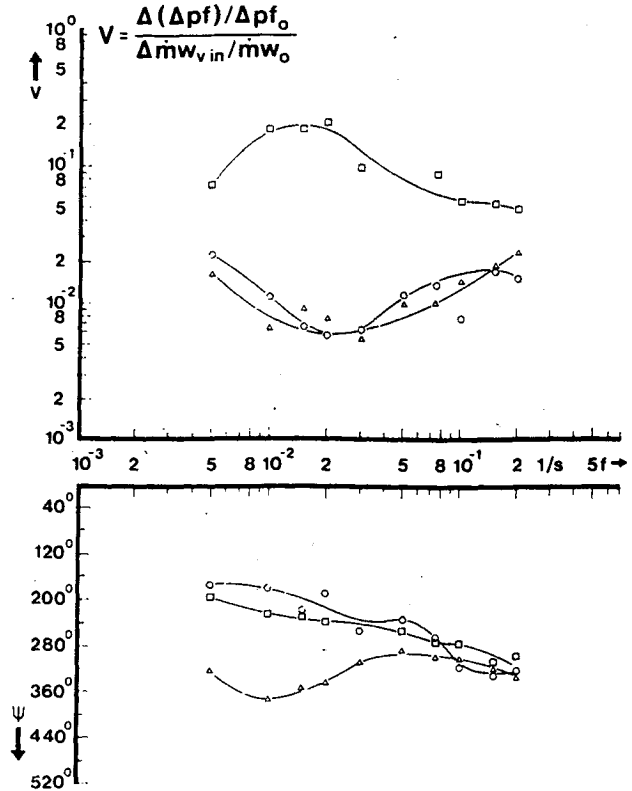
On both sides of the heat exchangers, at the inlet and outlet, measurements of the mass flow, the pressures and the temperatures were carried out. Stationary and transient measurements of the differential pressures were also taken. The pressures were determined by electrical pressure gauges and the temperatures by thermocouples. On the evaporation side the single phase mass flow was measured at the inlet and the two-phase mass flow at the outlet by turbine flow meters. In (10) a method is described for determining the two-phase mass flow. A theoretical investigation



Parameter

$\dot{m}w_o = 18 \text{ kg/m}^2\text{s}$ $p_{w_{in}o} = 0,46 \text{ bar}$ $\Delta \dot{m}w_{v_{in}} = 7,5 \text{ kg/m}^2\text{s}$
 $\diamond m_{f_o} = 600 \text{ kg/m}^2\text{s}$ $p_{f_{in}o} = 18,0 \text{ bar}$ $\Delta \vartheta_{f_{in}o} = 12^\circ\text{C}$
 $\triangle m_{f_o} = 1200$ "
 $\square m_{f_o} = 1500$ "
 $\circ m_{f_o} = 1800$ "

Fig. 9 Transfer functions of the test section in relation to the mass flow rate of condensate at the exit



Parameter

$\dot{m}w_o = 18 \text{ kg/m}^2\text{s}$ $p_{w_{in}o} = 0,46 \text{ bar}$ $\Delta \dot{m}w_{v_{in}} = 7,5 \text{ kg/m}^2\text{s}$
 $m_{f_o} = 1200 \text{ kg/m}^2\text{s}$ $\square p_{f_{in}o} = 15,0 \text{ bar}$ $\Delta \vartheta_{f_{in}o} = 12^\circ\text{C}$
 $\triangle p_{f_{in}o} = 16,5$ "
 $\circ p_{f_{in}o} = 18,0$ "

Fig. 10 Transfer functions of the test section in relation to the pressure drop on the evaporating side

of single phase flow shows that the turbine impeller is mainly driven by the momentum of the flow, while the shear stress and consequently the friction on the turbine vanes may be neglected.

For a two-phase flow the momenta of vapor and liquid are added to a total momentum

$$\dot{M}_{f_{lv}} w_{f_{lv}} = \dot{M}_{f_l} w_{f_l} + \dot{M}_{f_v} w_{f_v} \quad (1)$$

inducing the rotation of the turbine wheel. When inserting in equation (1) for the velocity of flow of the respective phase

$$w_{f_v} = \dot{M}_{f_v} / g f_v A f_v \quad (2)$$

$$w_{f_l} = \dot{M}_{f_l} / g f_l A f_l$$

and the definitions for the void fraction and quality, the result of the two-phase total mass flow is

$$\dot{M}_{f_{lv}} = w_{f_{lv}} A t f m \left(\frac{\dot{x} f^2}{\varepsilon f g f_v} + \frac{(1 - \dot{x} f)^2}{(1 - \varepsilon f) g f_l} \right) \quad (3)$$

The expression in the brackets is the reciprocal value of the average density, also called momentum density (11). The quality $\dot{x} f$ and the void fraction εf is seen in equation (3). For measuring the void fraction the gamma ray technique was applied. The vapor mass flow results from the following equation:

$$\dot{M}_{f_v} = \dot{x} f \cdot \dot{M}_{f_{lv}} \quad (4)$$

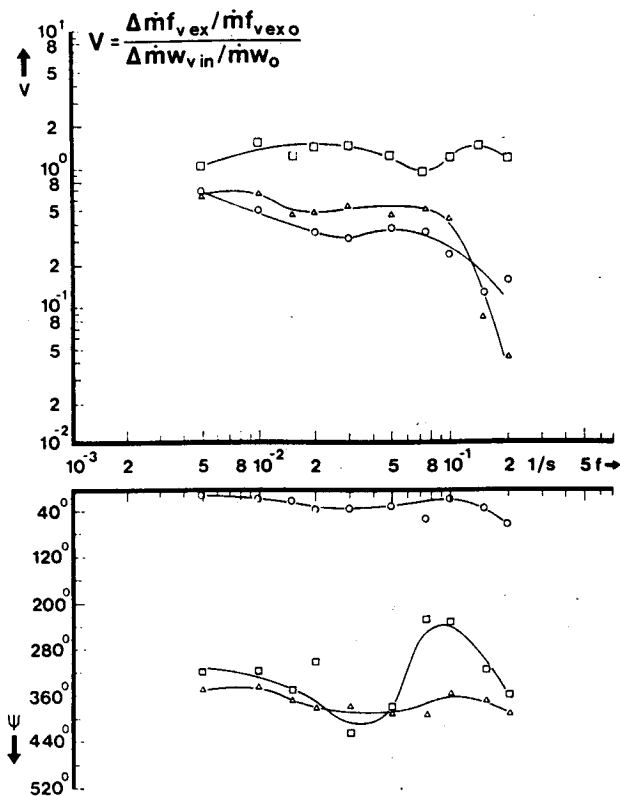
The quality in steady state can be determined by a conservation of energy out of the condensate mass flow:

$$\dot{x} f = \frac{\dot{Q}_o - c_{pf} \dot{M}_{f_o} \Delta \vartheta_{f_{in}o}}{\Delta h_{f_{lv}} \dot{M}_{f_o}} \quad (5)$$

with

$$\dot{Q}_o = \dot{M}_{w_{l_{exo}}} (\Delta h_{w_{lv}} + c_{pw} \Delta \vartheta_{w_{exo}}) \quad (6)$$

For transient condition this is not possible without knowing the slip. The slip $s f$ is defined as follows:



Parameter

$\dot{m}w_o = 18 \text{ kg/m}^2$ $p_{w_{in}} = 0.46 \text{ bar}$ $\Delta \dot{m}w_{vin} = 75 \text{ kg/m}^2$
 $\dot{m}f_o = 1200 \text{ kg/m}^2$ $\square p_{f_{in}} = 15.0 \text{ bar}$ $\Delta \dot{f}_{in} = 12^\circ\text{C}$
 $\Delta p_{f_{in}} = 16.5$ "
 $\circ p_{f_{in}} = 18.0$ "

Fig. 11 Transfer functions of the test section in relation to the mass flow rate of vapor at the exit

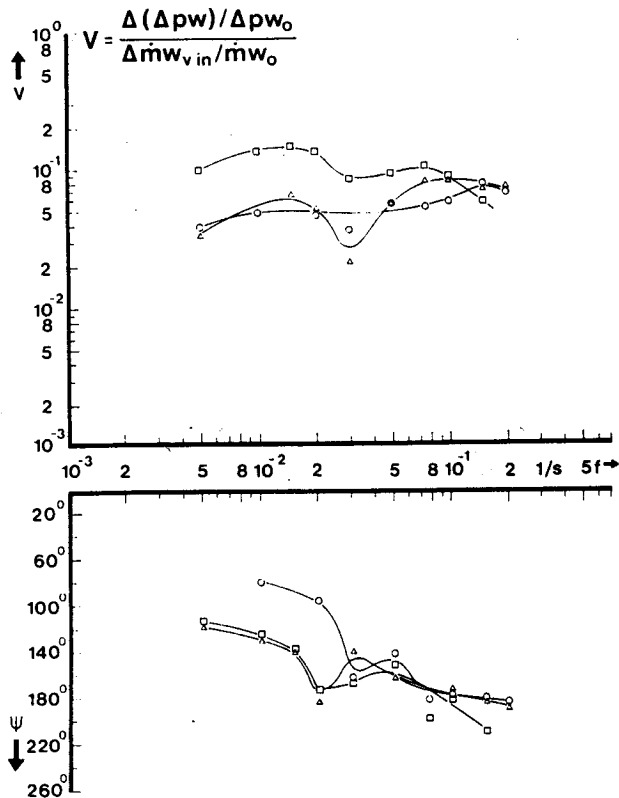
$$sf = \frac{1 - \epsilon f}{\epsilon f} \cdot \frac{\dot{x}f}{1 - \dot{x}f} \cdot \frac{qf_l}{qf_v} \quad (7)$$

The experiment with the lowest inlet subcooling $\dot{f}_{lin} = 4^\circ\text{C}$, where the slip was $sf = 1.4$, was an exception. The flow patterns in all these experiments were bubble flow and churn flow. At the inlet subcooling of $\dot{f}_{lin} = 4^\circ\text{C}$ the flow appears to change over into an annular flow. It may be assumed that the transient slip hardly differs from the slip measured in steady state, in so far as there are no instabilities or a change in flow pattern, differences up to 15 % may be possible.

The transient quality was therefore determined by the measured transient void fraction and the slip in steady state.

$$\dot{x}f = \frac{\epsilon f qf_v}{qf_l(1 - \epsilon f) + \epsilon f qf_v} \quad (8)$$

The condensate mass flow was directly measured



Parameter

$\dot{m}w_o = 18 \text{ kg/m}^2$ $p_{w_{in}} = 0.46 \text{ bar}$ $\Delta \dot{m}w_{vin} = 75 \text{ kg/m}^2$
 $\dot{m}f_o = 1200 \text{ kg/m}^2$ $\square p_{f_{in}} = 15.0 \text{ bar}$ $\Delta \dot{f}_{in} = 12^\circ\text{C}$
 $\Delta p_{f_{in}} = 16.5$ "
 $\circ p_{f_{in}} = 18.0$ "

Fig. 12 Transfer functions of the test section in relation to the pressure drop on the condensing side

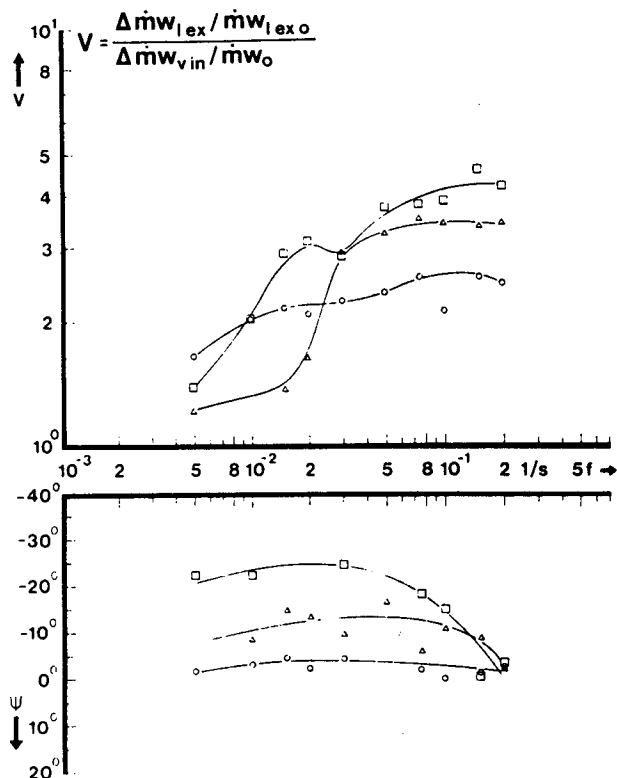
in steady state. The transient condition was determined out of the difference between the inlet and the outlet steam mass flow.

$$\frac{d\dot{M}_{st}}{dt} = \dot{M}_{w_{in}} - \dot{M}_{w_{ex}} - \dot{M}_{w_{lex}} \quad (9)$$

The measurements and calculations showed that the steam mass stored in the system is by one order of magnitude smaller than the oscillations of the condensate mass flow. The stored quantity was therefore neglected. The inlet and the outlet steam mass flow were measured with venturi tubes (11).

Representation of Results

For control actions in the linear system the superposition theorem is applicable, i.e. a doubling of the input signal is followed by a doubling of the output signal. The transient condition of a heat exchanger with double phase change is described by non-linear partial differential equations. The transfer function of a non-linear component, however,



Parameter

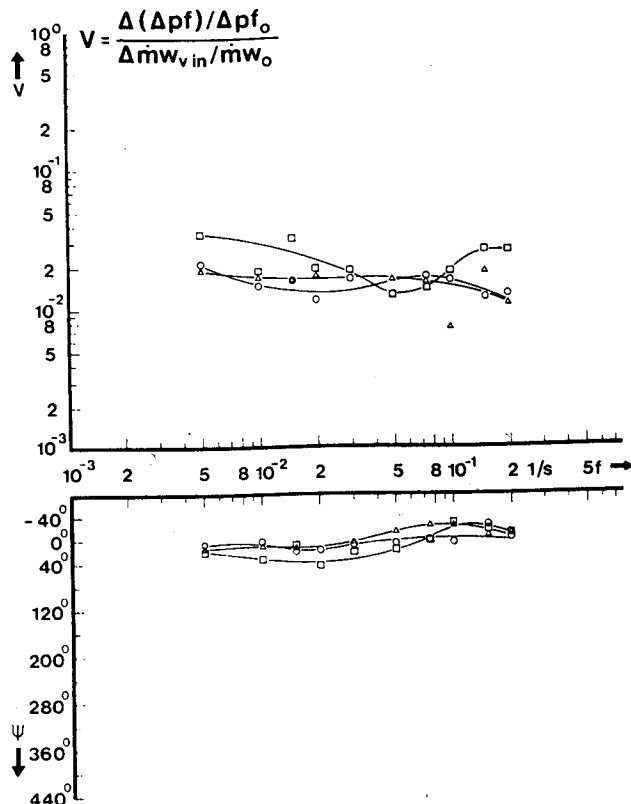
$\dot{m}w_0 = 18 \text{ kg/m}^2\text{s}$ $p_{w_{in}0} = 0.46 \text{ bar}$ $\Delta \dot{m}w_{vin} = 7.5 \text{ kg/m}^2\text{s}$
 $m_{f0} = 1200 \text{ kg/m}^2\text{s}$ $\square p_{f_{in}0} = 15.0 \text{ bar}$ $\Delta \Delta f_{in0} = 12^\circ\text{C}$
 $\Delta p_{f_{in}0} = 16.5$ "
 $\square p_{f_{in}0} = 18.0$ "

Fig. 13 Transfer functions of the test section in relation to the mass flow rate of condensate at the exit

is dependent on the amplitude of the input quantity. Due to the influence of the non-linearity, the oscillation of the response quantities is no longer purely sinusoidal. According to Fourier, each periodical shape of a curve can be represented as a superposition of single oscillations consisting of a basic oscillation ω and high-frequency harmonic oscillations 2ω , 3ω ... The analysis of the experiments showed that the basic oscillation reproduces the physical conditions of the single measured variables in an adequate accuracy. Based on this fundamental oscillation, the results for non-linear components - as well as for linear components - can be shown in the amplitude and phase transfer function. But here the transfer function does not only depend on the frequency but also on the amplitude of the inlet oscillation.

Analysis of the Experimental Results

During the oscillation experiments it could be seen that all inlet and outlet quantities, with the exception of the steam mass flow - the disturbed quantity -, tended towards a new quasi steady state value and os-



Parameter

$\dot{m}w_0 = 18 \text{ kg/m}^2\text{s}$ $p_{w_{in}0} = 0.46 \text{ bar}$ $\Delta \dot{m}w_{vin} = 7.5 \text{ kg/m}^2\text{s}$
 $m_{f0} = 1500 \text{ kg/m}^2\text{s}$ $\square p_{f_{in}0} = 18.0 \text{ bar}$ $\square \Delta f_{in0} = 4^\circ\text{C}$
 $\Delta \Delta f_{in0} = 8^\circ\text{C}$
 $\circ \Delta f_{in0} = 12^\circ\text{C}$

Fig. 14 Transfer functions of the test section in relation to the pressure drop on the evaporating side

cillated about it.

In Fig. 6 - 17 the absolute value of the transfer function is shown in dimensionless form. It is defined as follows:

$$|F| = V = \frac{\Delta y / y_0}{\Delta x / x_0} \quad (10)$$

and is also called amplification coefficient. The phase angle ψ can be determined from the difference between the two zero passages of the exciting oscillation and the response oscillation. When the oscillation of response lags behind the exciting oscillation, the phase angle is defined as positive.

Fig. 3 is a copy of a recording of the light beam oscilloscope. The figure shows the response of some thermodynamic and hydrodynamic parameters to a periodic exciting oscillation, which is caused by the steam mass flow at the inlet. This script refers only to a time of oscillation of 13 s, since the oscillating characteristics change with the oscillation time. The recording is necessary for the determination of the amplitudes and

Table 2 The experimental results of the steady states

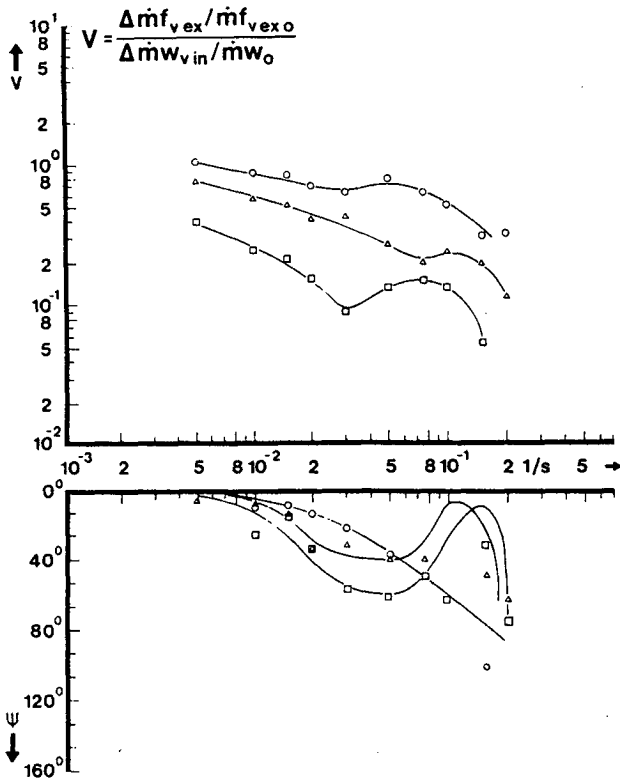
Exp. No.	\dot{m}_{f_0} kg/m ² s	$p_{f_{in0}}$ bar	Δp_{f_0} bar	$\vartheta_{f_{in0}}$ °C	$\vartheta_{f_{exo}}$ °C	$\Delta \vartheta_{f_{in0}}$ °C	\dot{m}_{w_0} kg/m ² s	$p_{w_{in0}}$ bar	Δp_{w_0} bar	$\vartheta_{w_{in0}}$ °C	$\vartheta_{w_{exo}}$ °C	$\dot{m}_{w_{lexo}}$ kg/m ² s	$\varepsilon_{f_{exo}}$	$\Delta \dot{m}_{w_{vin}}$ kg/m ² s
1	600.0	18.0	0.178	56.1	67.7	12.0	18.0	0.46	0.030	78.4	76.7	6.78	0.74	7.5
2	1200.0	18.0	0.222	56.1	67.0	12.0	18.0	0.46	0.040	79.2	77.0	7.12	0.46	7.5
3	1500.0	18.0	0.242	56.1	66.0	12.0	18.0	0.46	0.034	79.1	77.2	7.26	0.29	7.5
4	1800.0	18.0	0.263	56.1	65.5	12.0	18.0	0.46	0.031	78.9	77.2	7.63	0.18	7.5
5	1200.0	15.0	0.236	47.0	59.3	12.6	19.0	0.45	0.040	78.5	76.2	4.26	0.03	7.5
6	1200.0	16.5	0.236	51.8	62.9	12.2	18.4	0.46	0.032	78.5	76.7	5.21	0.22	7.5
11	1500.0	18.0	0.202	60.0	67.1	8.1	18.3	0.49	0.033	79.4	77.6	8.44	0.43	7.5
12	1500.0	18.0	0.192	63.9	67.6	4.2	17.2	0.48	0.029	79.4	77.8	8.09	0.59	7.5

the phase angles.

For the study of the feedback effects on heat exchangers with double phase change the hydrodynamic and thermodynamic parameters of the undisturbed evaporation side - as mass flow, pressure, and inlet subcooling - were varied. The influence of these parameters shall now be discussed.

Dependence on Mass Flow Rate of Freon.

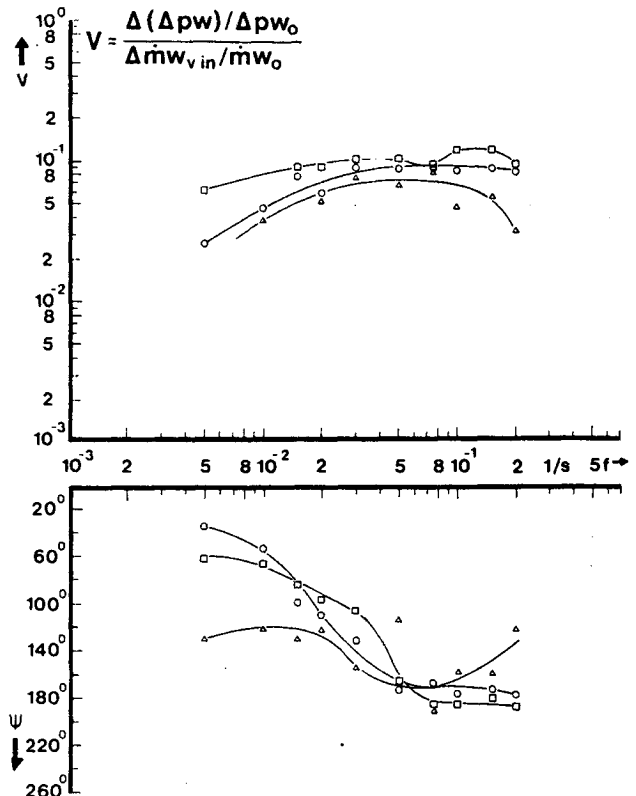
Fig. 6 shows the amplitude transfer function and phase angle transfer function as to the pressure drop on the evaporating side. With an increasing steam mass flow the heat transfer is improved on both sides. On the condensing side it is improved by an increase of the shear stress between steam and condensate



Parameter

$\dot{m}_{w_0} = 18 \text{ kg/m}^2\text{s}$ $p_{w_{in0}} = 0.46 \text{ bar}$ $\Delta \dot{m}_{w_{vin}} = 7.5 \text{ kg/m}^2\text{s}$
 $\dot{m}_{f_0} = 1500 \text{ kg/m}^2\text{s}$ $p_{f_{in0}} = 18.0 \text{ bar}$ $\square \Delta \vartheta_{f_{in0}} = 4^\circ\text{C}$
 $\triangle \Delta \vartheta_{f_{in0}} = 8^\circ\text{C}$
 $\circ \Delta \vartheta_{f_{in0}} = 12^\circ\text{C}$

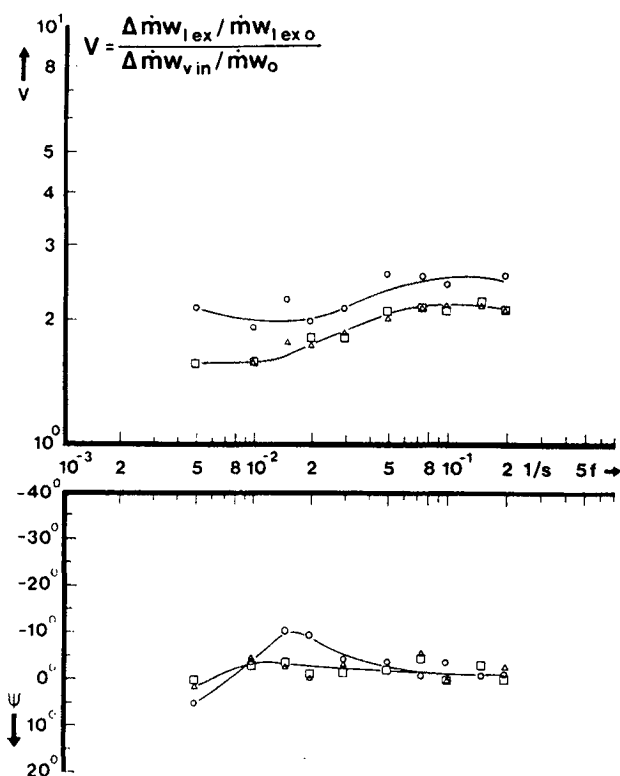
Fig. 15 Transfer functions of the test section in relation to the mass flow rate of vapor at the exit



Parameter

$\dot{m}_{w_0} = 18 \text{ kg/m}^2\text{s}$ $p_{w_{in0}} = 0.46 \text{ bar}$ $\Delta \dot{m}_{w_{vin}} = 7.5 \text{ kg/m}^2\text{s}$
 $\dot{m}_{f_0} = 1500 \text{ kg/m}^2\text{s}$ $p_{f_{in0}} = 18.0 \text{ bar}$ $\square \Delta \vartheta_{f_{in0}} = 4^\circ\text{C}$
 $\triangle \Delta \vartheta_{f_{in0}} = 8^\circ\text{C}$
 $\circ \Delta \vartheta_{f_{in0}} = 12^\circ\text{C}$

Fig. 16 Transfer functions of the test section in relation to the pressure drop on the condensing side



Parameter

$\dot{m}_{w0} = 18 \text{ kg/m}^2\text{s}$ $p_{w\text{in}0} = 0.46 \text{ bar}$ $\Delta \dot{m}_{w\text{in}} = 7.5 \text{ kg/m}^2\text{s}$
 $\dot{m}_{f0} = 1500 \text{ kg/m}^2\text{s}$ $p_{f\text{in}0} = 18.0 \text{ bar}$ $\square \Delta f_{\text{in}0} = 4^\circ\text{C}$
 $\triangle \Delta f_{\text{in}0} = 8^\circ\text{C}$
 $\circ \Delta f_{\text{in}0} = 12^\circ\text{C}$

Fig. 17 Transfer functions of the test section in relation to the mass flow rate of condensate at the exit

film, and on the evaporating side by an increase of quality. When the steam mass flow is varied periodically at the inlet and when the mass flow at the inlet of the evaporating side is constant, periodical density oscillations appear on this side. The smaller the frequency of the exciting oscillation, the larger the amplitudes and the smaller the phase angles of the differential pressure oscillations. The largest amplification coefficient of the differential pressure is at the smallest mass flow $\dot{m}_f = 600 \text{ kg/m}^2\text{s}$. There are two reasons for this: First, the steady state pressure drop of $\dot{m}_f = 600 \text{ kg/m}^2\text{s}$ is the smallest (Table 2). Second, at small mass flows, the periodical steam mass flow oscillations lead to larger average density oscillations. The pressure drop on the evaporating side is the sum of the geodetical, momentum, and friction pressure drop. An increase of the steam mass flow causes a decrease of the average density on the evaporating side. A smaller average density entails a decrease of the geodetic pressure drop, an increase of the momentum pressure drop, and

an increase of the friction pressure loss. The geodetic pressure drop oscillation is dephased by 180 degrees in regard to the momentum pressure drop and the friction pressure loss oscillation, i.e. interferences are possible. At mass flows $\dot{m}_f = 600$ and $1200 \text{ kg/m}^2\text{s}$ the amplitude of the geodetical pressure drop oscillation is larger than the sum of the amplitudes of momentum pressure drop and friction pressure loss oscillations. With decreasing frequency the phase angle tends to 180 degrees. When the sum of amplitudes of the momentum pressure drop and friction pressure loss oscillations is larger, as is the case with the mass flows $\dot{m}_f = 1500$ and $1800 \text{ kg/m}^2\text{s}$, the phase angle tends towards zero with decreasing frequency. In all four of the mass flows in fig. 6 the flow will be unstable within a definite frequency range. The limits of the range of instability result from the minima or maxima of the amplitude or phase transfer function respectively. The instability is probably caused by a change of the flow pattern. In Fig. 4 (12) the steady points of operation are marked and the flow patterns of the test series can be recognized. The mass flow $\dot{m}_f = 1800 \text{ kg/m}^2\text{s}$ is stable for the total frequency range. The point of operation is in the range of bubble flow. This range is not left in non-steady state operation. The operation points of the mass flows $\dot{m}_f = 1500$ and $1200 \text{ kg/m}^2\text{s}$ are still in the range of bubble flow. In non-steady state operation, however, there is not only bubble flow but also transition flow between bubble and annular flow. The instability appears because a bubble flow has a better heat transfer and a higher pressure drop than an annular flow.

In the following the transfer function in regard to the differential pressure drop at a mass flow of $\dot{m}_f = 1200 \text{ kg/m}^2\text{s}$ shall be explained in detail. In the frequency range from 0.005 Hz to 0.02 Hz there is an annular flow. The amplification decreases with an increase in frequency and the phase angle becomes larger. Bubble flow develops within a frequency of $f \geq 0.15 \text{ Hz}$. The maximum of the amplification starts at $f = 0.15 \text{ Hz}$, since the pressure drop and the heat transfer of a bubble stream are higher than those of an annular flow. As the phase shift of a bubble flow is smaller than that of an annular flow, it drops to a minimum at a frequency of $f = 0.15 \text{ Hz}$. For the frequency range $0.005 < f < 0.15$ there is a transition flow between bubble and annular flow. The frequency range of the transition flow is extended when the steady state operation point borders on one of the boundary curves of bubble churn flow or churn-annular flow (see Fig. 4). When the steady state operation point of a flow is in the range of the churn-flow, this may result in unstable characteristics in the non-steady state operation, although this is not always the case. The mass flow $\dot{m}_f = 600 \text{ kg/m}^2\text{s}$ is unstable only in the frequency range of $0.026 < f < 0.05$. This range is not always reproducible. In spite of the churn-flow the mass flow $\dot{m}_f = 600 \text{ kg/m}^2\text{s}$ shows stable characteristics in a large frequency range.

In Fig. 7 the amplitude transfer function and phase transfer function in relation

to the vapor mass flow at the outlet on the evaporating side are marked. The transfer functions in regard to the differential pressure and the vapor mass flow on the evaporating side have almost the same instability ranges. This can be traced back to the close coupling of the thermodynamic and hydrodynamic parameters such as mass flow, pressure drop, and heat transfer. For the amplitude transfer function as to the vapor mass flow with the parameter $mf_0 = 600 \text{ kg/m}^2\text{s}$ there is a long sloping curve for the frequency $f < 0.05 \text{ Hz}$. This can be explained by the fact that the controller action of a heat exchanger with double phase change is comparable with the controller action of a linear controlled system showing PT_2 characteristics. Fig. 5 represents the transient response and the transfer function of a linear controlled system with PT_2 characteristics, and can be compared with Fig. 6 - 17. The mass flow $mf_0 = 600 \text{ kg/m}^2\text{s}$ has a high void fraction. Therefore, the feedback effect between the condensing and evaporating sides is very strong. On the one hand, oscillations with damping $D < 1$ are possible, on the other hand, the store capacity of the heat exchanger becomes higher with increasing void fraction. The void fraction is an important determinant of the dead time characteristics of a plant. A high void fraction causes a strong increase of the phase shift, especially at high frequencies.

Fig. 8 shows the amplitude and phase transfer function in relation to the differential pressure on the condensing side. As the transit time of a fluid particle is by one order of magnitude smaller than the smallest oscillation time, all transient procedures on this side are to be traced back to the feedback of the condensing and the evaporating side. Those feedback effects which produce instabilities on the evaporating side may also produce instabilities on the condensing side or vice versa. But instabilities on the one side can also be damped by the other side or even cancelled. The mass flow $mf_0 = 1500 \text{ kg/m}^2\text{s}$ may serve as an example. Those mass flow instabilities appear within a small frequency range on the evaporating side for both the transfer function in relation to the vapor mass flow as well as the differential pressure. Due to the damping effect of the tube wall and the condensate film, this mass flow shows no instabilities in the transfer function with regard to the differential pressure.

A comparison of the transfer functions between evaporating and condensing side shows that the amplitude transfer function on the evaporating side decreases with increasing frequency and that on the condensing side the amplitude transfer function first increases from lower to higher frequencies and then decreases. Exceptions are the ranges of instability and the transfer function with the parameter $mf_0 = 600 \text{ kg/m}^2\text{s}$. This can be explained by looking at the response $D < 1$ of a linear control section shown in Fig. 5. A sudden increase of the steam mass flow entails a delayed increase of the differential pressure. When the geodetical pressure drop is neglected, then the pressure drop is the dif-

ference between friction pressure drop and momentum pressure drop. An increased steam mass flow improves the heat transfer on the condensing side. Thereby more vapor is produced on the evaporating side and the two-phase heat transfer grows. This increased heat transfer, results in more condensate and an increase of the momentum pressure drop on the condensing side. The total pressure drop decreases again.

In principle, instabilities on the condensing side may have the same causes as those on the evaporating side. In the present case it is mainly a question of density oscillations. Within practically the same frequency range, where instabilities arise on the evaporating side, they are also apparent on the condensing side. By improved heat transfer more condensate is produced on the condensing side, when there is a transition from annular flow to bubble flow on the evaporating side. The periodical steam mass flow effect an alternating acceleration and deceleration of the condensate mass flow. An additional mass of condensate requires a corresponding pressure drop, i.e. the amplification coefficient of the differential pressure rises.

Fig. 8 shows the transfer function of amplitude and phase in relation to the condensate mass flow. Here the phase transfer function is remarkable, as the phase angles are ranging around 0 degrees. The difference between the highest and lowest phase shifting is 20 degrees. As the error in the phase shifting may be as much as 10 degrees, a common fitting curve has been chosen for all measuring points. Each change of the steam mass flow at the inlet of the test section is connected with a change in pressure. As the steam is in a saturated state, the temperature has to change, too. When the steam mass flow increases, the difference in temperature between steam and condensate film also increases. As a consequence, more steam is condensed. As the passage time of the condensate through the test section is by one order of magnitude smaller than the shortest time of oscillation, the phase angle of the condensate mass flow for low and high frequencies is zero. For medium frequencies even negative phase angles are possible. Although the steam mass flow decreases after passing its maximum, the temperature difference between steam and condensate still increases for a short time due to the feedback coupling between the condensing and the evaporating sides. At this moment the condensate film gives off more heat to the evaporating side than it receives from the condensing side.

Dependence on Pressure of Freon. Fig. 10 to 13 illustrate the transfer as a function of the pressure of the evaporating side. A lowering of the pressure on the evaporating side causes, under the same conditions on the condensing side, an increase of the temperature difference between both sides. Table 2 shows that despite an increase of the temperature difference between the condensing and evaporating sides the exchanged heat decreases. The causes lie on the evaporating side.

The high difference in temperature between tube wall and freon leads to a dry-out. The oscillation of the steam mass flow results in periodical changes of the heat transfer on the condensing side and in oscillations of temperature of the tube wall. Thereby a re-wetting of the tube wall in the range of instability takes place on the evaporating side. This effect is not characteristic of heat exchangers with double phase change, but occurs when condensing steam freon evaporates. Fig. 10 illustrates that at a film boiling the phase angles tend towards 270 degrees for low frequencies, i.e. when the steam mass flow reaches its minimum, the heat transfer is best on the evaporating side.

Dependence on the Subcooling at the Inlet of Freon. When studying the stability as a function of the subcooling at the inlet, the same flow mechanisms as used in the study of stability as a function of the mass flow may be taken for a basis. In both cases the void fraction is changed. Only at a variation of the subcooling at the inlet the length of the evaporation part changes. The evaporation length influences the time of passage of a fluid particle. This time, however can be disregarded, as it is by one order of magnitude smaller than the shortest time of oscillation. As with the variation of mass flow the stability of the system essentially depends on the position of the operation point in the flow pattern map. Pure bubble flows or pure annular flows tend less to instabilities than flows in the transition region. Fig. 14 - 17 show the influence of the subcooling at the inlet on the transfer function. By Fig. 4 it becomes obvious that the steady operation points are in the transition region between the bubble flow and annular flow. The smaller the subcooling at the inlet, the more the flow differs from a bubble flow. But the flow is not yet an annular flow. With a decrease in the subcooling the frequency range where instabilities occur increases, and the difference between the maximum and minimum amplification coefficient grows.

CONCLUSION

During the operation of a heat exchanger with double phase change instabilities may arise due to external perturbations. As a two-phase mixture flows on both the condensing side and the evaporating side, there are strong feedback effects between both. Instabilities on one side have a damping or an amplifying effect on the other side. The range of instabilities is limited by significant minima and maxima in the transfer functions of amplitude and phase. The instabilities arise principally from the same mechanisms on both sides of the heat exchanger. On the condensing side, the reasons for instabilities are mainly density oscillations, on the evaporating side, a change of the flow pattern or instable film boiling.

ACKNOWLEDGMENTS

The research described in this paper was

carried out under the sponsorship of SFB 61, "Strömungsprobleme in der Energieumwandlung", under Grant 2000/61/74 (E7).

REFERENCES

- 1 Bergles, A.E., "Review of Instabilities in Two-Phase Systems," Proceedings of the NATO Advanced Study Institute on Two-Phase Flows and Heat Transfer, Istanbul, Aug. 1976.
- 2 Bouré, J.A., Bergles, A.E., Tong, L.S., "Review of Two-Phase Flow Instability," Nuclear Engineering and Design, Vol. 25, 1973, pp. 165-192.
- 3 Grant, I.D.R., "Shell-and-Tube Heat Exchangers for the Process Industries," Chemical Processing, Dec. 1971, pp. 58-65.
- 4 Fabrega, S., "Etude Experimentale des Instabilités Hydrodynamiques Survenant dans les Réacteurs Nucléaires a Ebullition," CEA-R-2884, 1964.
- 5 Jeglic, F.A., Grace, T.M., "Onset of Flow Oscillations in Forced-Flow Subcooled Boiling," NASA-TN-D 2821, 1965.
- 6 Stenning, A.H., Veziroglu, T.N., "Flow Oscillations Modes in Forced Convection Boiling," Proceedings of the 1965 Heat Transfer and Fluid Mechanics Institute, Stanford Univ. Press, 1965, pp. 301-316.
- 7 Wedekind, G.L., Bhatt, B.L., Beck, B.T., "A System Mean Void Fraction Model for Predicting various Transient Phenomena Associated with Two-Phase Evaporating and Condensing Flows," Proceedings of the NATO Advanced Study Institute on Two-Phase Flows and Heat Transfer, Istanbul, Aug. 1976.
- 8 Mathisen, R.P., "Out of Pile Channel Instability in the Loop Skolvan," Euratom Report, Symposium on Two-Phase Dynamics, Vol. 1, Eindhoven, Sept. 1967, pp. 19-64.
- 9 Crowley, J.D., Deane, C., Gouse, S.W., "Two-Phase Flow Oscillations in Vertical Parallel Heated Channels," Euratom Report, Symposium on Two-Phase Dynamics, Vol. 2, Eindhoven, Sept. 1967, pp. 1131-1171.
- 10 Belda, W., "Dryoutverzögerung bei Kühlmittelverlust in Kernreaktoren," Dissertation am Institut für Verfahrenstechnik der Technischen Universität Hannover, 1975.
- 11 Heckle, M., "Bestimmung der Zweiphasenströmung Gas/Flüssigkeit durch Drosselorgane," Chemie-Ingenieur-Technik, 42. Jahrgang, Nr. 5, 1970, pp. 304-310.
- 12 Zetzmann, K., Mayinger, F., "Flow Pattern of Two-Phase Flow Inside Cooled Tubes," Proceedings of the NATO Advanced Study Institute on Two-Phase Flows and Heat Transfer, Istanbul, Aug. 1976.